Daagu International Journal of Basic and Applied Research 7(1) (2025): 662-681

Research article

Google Earth Engine Based Soil Loss Estimation in Eastern Tigray Zones, Ethiopia

Fikre Belay Tekulu (PhD) [1], Zubairul Islam (PhD) [2], Haftom Teshale Gebre[3], and Tadesse Brhane Hadgu[4]

[1]Department of Geography and Environmental Studies, CSSH, Adigrat University, Tigray, Ethiopia. fikrebelay23@gmail.com
[2]Department of Management, Abuja University, Nigeria zubairul@gmail.com
[3]Department of Geography and Environmental Studies, CSSH, Adigrat University, Tigray, Ethiopia. E-mail address: haftomteshale1@gmail.com
[4]Department of Geography and Environmental Studies, CSSH, Adigrat University, Tigray, Ethiopia. E-mail: tadesse1985@gmail.com
Corresponding author: fikrebelay@gmail.com

Received: December 16, 2024 Revised: March 19, 2025 Accepted: March 26, 2025

Abstract

Soil loss and its geostatistical analysis was studied at the kebele level in Tigray. The method applied to estimate soil loss was the revised universal soil loss equation. Earth Engine's public data archive was used for data collection. The R factor was developed from the SM2RAIN-ASCAT (2007-2021) global daily satellite rainfall data, the K-factor was developed from USDA-3A1A1A_M/v02 soil data, the C-factor was derived from MODIS/006/MOD13A2, and LS factor was derived from WWF Hydro SHEDS Hydrologically Conditioned DEM. By integrating all factors, the soil loss was obtained by the RUSLE model. Spatial Autocorrelation (Morans I) statistic was used to identify the pattern of soil loss and Ordinary Least Squares (OLS) linear regression was used to model a soil loss in terms of its relationships to R, K, LS, C, and P factors. The grouping analysis tool was used to Group kebele based on soil loss. The results indicate that the estimated average soil erosion is 82760 t ha^{-1} y^{-1}. The pattern of soil loss at the kebele level was found highly clustered with a z-score of 23.39. The groping analysis tool divides the kebele into five categories to identify the cause of spatial variation of the soil loss in Tigray. Groups 1, 4 & 5 were found as in the outlier positions due to the high LS factor. The results deliver valuable information for decision-makers and planners to take suitable land administration measures to minimize the soil loss.

Keywords: RUSLE, GEE, Soil Erosion, OLS, Grouping Analysis

©*Daagu International Journal of Basic and Applied Research*

1. INTRODUCTION

Land degradation remains a critical global issue, especially in its role in exacerbating food insecurity. Over one billion people are food insecure (Kuria et al., 2018), and with the global population projected to reach 9 billion by 2050 (Rockström & Falkenmark, 2015), the pressure on land will only intensify. Deforestation and soil erosion are key contributors to land degradation, driven primarily by population growth and unsustainable agricultural expansion. Water erosion alone accounts for over 90% of soil erosion globally (Megerssa & Bekere, 2019). Though its effects accumulate gradually, soil erosion eventually leads to droughts, reduced crop yields, and famine (Tesfahunegn, 2020).

Sub-Saharan Africa, particularly Ethiopia, faces significant soil erosion challenges. More than 65% of the land in the region shows signs of degradation (Sileshi et al., 2019). In Ethiopia, soil erosion removes roughly two billion tons of soil annually—equivalent to a loss of one million tons of grain. This soil loss affects agricultural productivity by deteriorating soil properties such as organic matter, water content, and nutrient levels. Highland areas, especially in the Tigray region, are most affected due to steep slopes, intense rainfall, and minimal vegetation cover (Esser & Haile, 2002).

Tigray's semi-arid highlands experience high erosion rates due to frequent runoff from short but intense summer rains, deforestation for fuel, and conventional farming techniques. Only 15% of the region’s population has access to electricity, forcing rural communities to rely on wood, cow dung, and cover crops for fuel—practices that further degrade soil quality (Kaygusuz, 2011). The need to convert forest and marginal lands for agriculture has accelerated soil erosion, severely impacting food security.

Efforts to address soil erosion have included soil and water conservation programs, integrated watershed management, water harvesting, and conservation tillage. While these interventions, such as those in Abraha with Atsebha, have shown success at small scales (Tadesse et al., 2016), broader regional-scale data on soil loss is limited. Most studies focus on plot-level erosion, such as those by Govers and Moeyersons (2005), making it difficult to inform large-scale planning or policy.

To develop effective strategies, it is essential to estimate soil loss at the regional or zonal level. Understanding spatial variations in erosion can guide policy, prioritize intervention zones, and improve conservation outcomes. Erosion models play a vital role in estimating soil loss and informing sustainable land use decisions. Among these, the Revised Universal Soil Loss

Equation (RUSLE) is widely used due to its simplicity and adaptability to various landscapes (Wilken et al.,2020). RUSLE has been applied in many Ethiopian studies and is particularly suitable for Tigray's hilly terrain.

The model estimates soil erosion using five factors: rainfall erosivity (R), soil erodibility (K), slope length and steepness (LS), cover management (C), and conservation practices (P). Advances in GIS and remote sensing technologies have enhanced the accuracy and feasibility of using RUSLE at larger spatial scales. By incorporating high-resolution data such as digital elevation models (DEMs) and NDVI (Normalized Difference Vegetation Index) for land cover analysis, GIS-integrated RUSLE modeling can spatially identify erosion hotspots (Ganasri & Ramesh, 2016; Mitasova et al., 2013).

However, challenges remain, particularly in parameter estimation and data availability, especially for K and P factors. While empirical data are preferred, field-based validation remains essential to ensure the reliability of model predictions. As climate change intensifies rainfall patterns and increases erosion potential, tools like RUSLE, enhanced through GIS and remote sensing, will be increasingly crucial.

There have been relatively few regional studies in the Tigray regional state of Ethiopia on the use of RUSLE technologies for finding the kebele prone to more water erosion. This research focuses on applying geostatistical analysis combined with GIS-based RUSLE modeling to estimate soil loss in Tigray, Ethiopia. The aim is to inform more targeted soil conservation planning, improve food security, and support sustainable land management in one of the country's most erosion-prone regions.

The purpose of this is 1) to predict the soil erosion using RUSLE; 2) to predict the pattern of soil loss at the kebele level in Tigray Region; and 3) to exercise linear regression to understand the impact of variables of soil loss and the last to group the kebele based on soil loss estimation.

2. MATERIAL AND METHODS

2.1. Study Area

Eastern Tigray Zone is located in the northern part of Ethiopia and is composed of 18 woredas, with a total area of 6,392 km^2. It is located between 13°32'59"N up to 14°40'56"N and between 39°11'39"E up to 39°59'43"E longitude (Figure 1). Generally, this zone is bordered by Eritrea in the North, by the Central zone in the West, by the South Eastern in the South, and by the Afar regional State in the East.

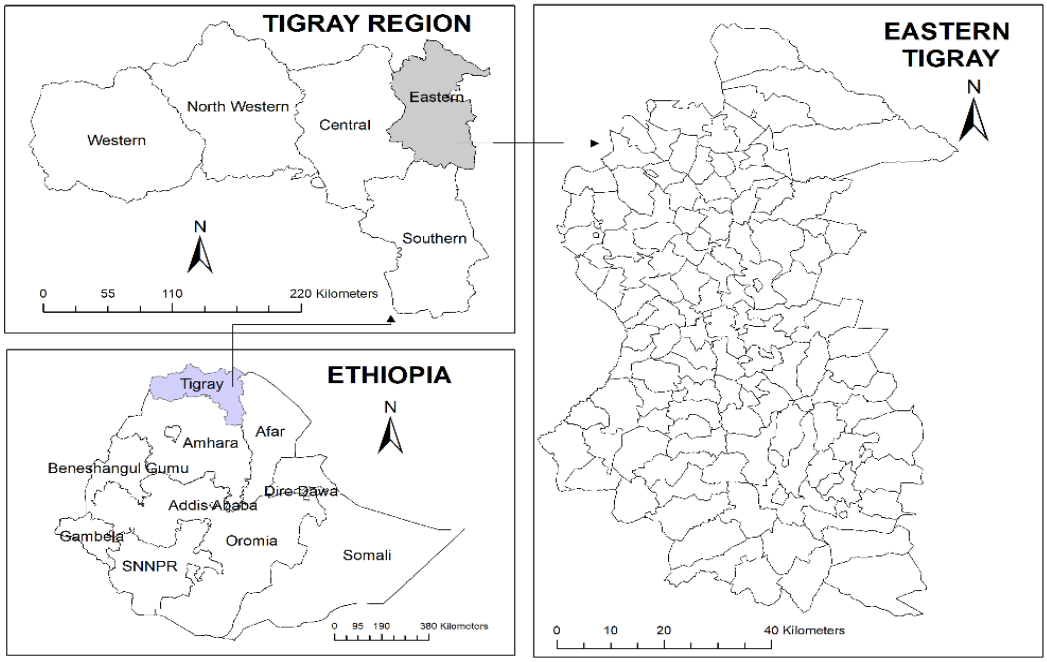


Figure 1. Study Area Map

2.2. Topography of the Study Area The elevation of the study area ranges from its lowest 148 meters above sea level up to 3,298 meters above sea level. Its mean elevation above sea level equals 2,225 meters. It is characterized by the local climate primarily 'degua', 'weyna degua' and 'kola.

2.3. Climate of the Study Area

The climate is commonly defined as the weather average over a long period mostly used for 35 years. Climate includes the statistics of temperature, humidity atmosphere pressure, wind, and precipitation. However, the data is limited to temperature and rainfall. These two climatic elements of the course are the most important for both agriculture and hydrology.

In Eastern Tigray, as in other parts of the country, the climate is determined by latitudinal and altitudinal factors. Annual rainfall of the zone ranges from its minimum in Erob about 140 mm up to the highest in Saesie-Tsaeda-Emba about 672mm. Similarly, with regard to temperature, the lowest temperature is experienced in Ganta Afeshum including Adigrat about 6°C up to the maximum of about 30°C in Erob (Adigrat University, 2018).

Several land use types including forests, croplands, built-up area, and exclosure areas exist in Tigray. Typical soil types in the region include, lithosols, cambisols, acrisols, vertisols luvisols, xerosols regosols, arenosols, fluvisols rendzinas nitosols(Gebregziabher et al., 2009) .Mixed farming system of crop farming with livestock production are typical farming practices in the region of which more than 90% of farming is practiced by small holder farming.(Zerssa et al., 2021). Agriculture is the mainstay economy in the region contributing to 60% of GDP. The

main crops grown in in the region are barley, maize, wheat, sorghum, Teff (Eragrostis tef), along with leguminous crops: chickpeas, field peas, and horse bean. Sheep, goat, Cattle, beehives, and chicken are common livestock reared in the zone.

2.4. Workflow

RUSLE is fit for the soil loss estimation model that can be used at any level of region (Ganasri & Ramesh, 2016). The workflow implemented in this study is given in Figure 2.

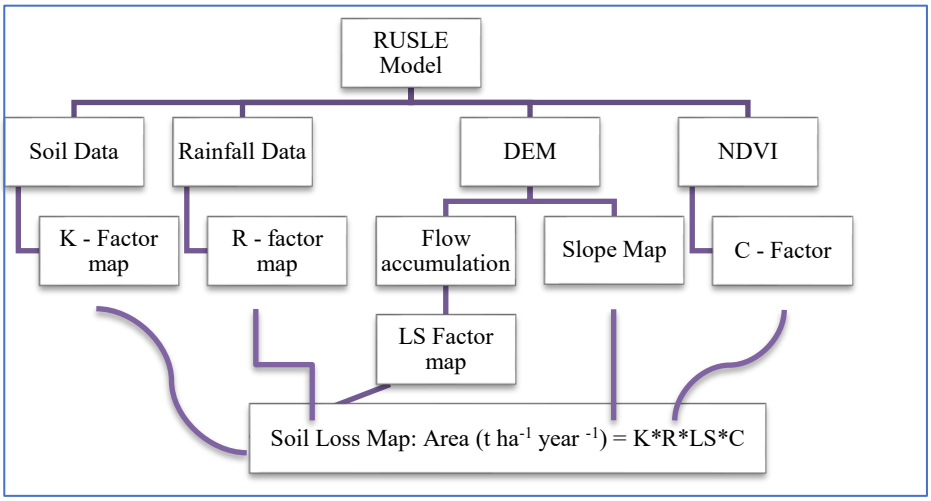


Figure 2. RUSLE Workflow chart

2.5. Data Used

The source and type of data used are given in Table 1.

Table 1. Data Types and sources

Dataset	Content	Format	Data Source
Precipitation	Monthly Rainfall in mm, one km spatial resolution, Covering Period 2007-2018.	tif	https://openlandmap.org/ (Brocca et al., 2019)
Soil	Sand, Silt, Clay, Organic Content	tif	https://openlandmap.org/
DEM	SRTM dataset with 1 km spatial resolution	tif	https://www.hydrosheds.org/
NDVI	The MODIS vegetation index (VI) products.	tif	https://lpdaac.usgs.gov/
Basic geographical information	Administrative Map	Vector	https://www.diva-gis.org/gdata

2.6. Data Processing

2.6.1 RUSLE

RUSLE, one of the foremost widely used models (Eq. 1), gives an idea of how to get the interaction between precipitation and soil erosion (Xu et al., 2013).

$$A = R * K * LS * C * P \quad (1)$$

where, R stands for precipitation runoff erosivity factor (MJ·mm·km−2·h−1·month−1); K is for the soil erodibility variable (t·km2·h·km−2 MJ−1·mm−1); LS is steepness and length of the slope factor (dimensionless); C is the factor for cover management (dimensionless); P is the erosion control practice factor (dimensionless, between 0 and 1) and A is the calculated soil loss (t·km−2·annum−1).

Rainfall factor (R): For the monthly R, it is calculated according to daily data or monthly data.

$$R = 1.73 * 10^{(1.5*log(\frac{Pm^2}{Pa})-0.08188)} \quad (2)$$

Where R is the erosivity by rainfall in MJ in mm /ha h^{-1} y^{-1}, Pm is the precipitation in the month and Pa is the precipitation in a year.

Box 1. shows the Java script used in GEE to find the R factor.

```
var Precipitation_E_Tigray=
ee.Image("OpenLandMap/CLM/CLM_PRECIPITATION_SM2RAIN_M/v01")

Var Annual Precipitation_ Tigray= Precipitation_ E_Tigray.reduce(ee.Reducer.sum())

Var Monthly_Precipitation_T_ Tigray=
ee.Image(10).pow(ee.Image(1.5).multiply(Precipitation_E_Tigray.pow(2).divide(Ann
ual_Precipitation_E_Tigray).log10().subtract(-0.08188))).multiply(1.735)

var factorR = Monthly_Precipitation_Tigray.reduce(ee.Reducer.sum())
```

Soil factor (K): It can be assessed using soil's texture and organic data (Sharpley and Williams, 1990).

$$K = [0.2 + 0.3 * exp - 0.0256 * SAN * (1 - SIL/100)] * [1 - \frac{0.25 * CLA}{CLA + exp(3.72 - 2.95 * CLA)}] \quad (3)$$

Where SAN is the sand percentage, SIL is the silt percentage and CLA is the clay percentage. Box 2 shows the Java script used in GEE to find the factor of soil erodibility (K).

Box 2. *GEE code for soil erosivity factor (K)*

```
var sand = ee.Image("OpenLandMap/SOL/SOL_CLAY-WFRACTION_USDA-3A1A1A_M/v02").select('b0')

var silt = ee.Image('users/aschwantes/SLTPPT_I').divide(100)

var clay = ee.Image("OpenLandMap/SOL/SOL_SAND-WFRACTION_USDA-3A1A1A_M/v02").select('b0')

var morg = ee.Image("OpenLandMap/SOL/SOL_ORGANIC-CARBON_USDA-6A1C_M/v02").select('b0').multiply(0.58)

var sn1 = sand expression('1 - b0 / 100', {'b0': sand})

var orgcar = ee.Image("OpenLandMap/SOL/SOL_ORGANIC-CARBON_USDA-6A1C_M/v02").select('b0')

var soil = ee.Image([sand, silt, clay, morg, sn1, orgcar]).rename(['sand', 'silt', 'clay', 'morg', 'sn1', 'orgcar'] )

var factor K = soil expression(

  '(0.2 + 0.3 * exp(-0.0256 * SAND * (1 - (SILT / 100)))) * (1 - (0.25 * CLAY / (CLAY + exp(3.72 - 2.95 * CLAY)))) * (1 - (0.7 * SN1 / (SN1 + exp(-5.51 + 22.9 * SN1))))',

  {'SAND': soil.select('sand'), 'SILT': soil.select('silt'), 'CLAY': soil.select('clay'), 'MORG': soil.select('morg'), 'SN1': soil.select('sn1'), 'CORG': soil.select('orgcar')

  });
```

LS factor: It is an accelerating factor for rainfall erosion. Moore (1985) developed the method of slope length. S is assessed by step coupling techniques (McCool. 1989; Liu.1994).

$$LS = (0.4 + 1) * (Flowacc * CellSize/22.13)^{0.4} * (sin\theta/0.0896)^{1.3} \quad (4)$$

Where LS is the horizontal length of the slope, Flowacc is the horizontal length of the slope θ is the slope of DEM (Degrees). Box 3 shows the Java script used in GEE to obtain the LS factor.

Box 1. GEE code for LS erosivity factor (LS)

```
Var facc = ee.Image("WWF/HydroSHEDS/15ACC")
Var dem = ee.Image("WWF/HydroSHEDS/03CONDEM")
Var slope = ee.Terrain.slope(dem)
Var ls_factors = ee.Image([facc, slope]).rename(['facc','slope'])
Var factorLS = ls_factors.expression(
 '(FACC*270/22.13)**0.4*(SLOPE/0.0896)**1.3',
 {
  'FACC': ls_factors.select('facc'),
  'SLOPE': ls_factors.select('slope')  });
```

C factor: It is related to cover management, which was calculated from the NDVI (Eq. 5) (appendixes Figure 6 Erosivity factor C)

$$NDVI = (NIR - Red)/(NIR + Red) \quad (5)$$

Where *Red* & *NIR* are the wavebands of EMR.

The technique (Eq. 6) for the C factor was used because the CrA is dependent on NDVI & tropical climate conditions (Almagro et al., 2019) (appendixes Figure 6 Erosivity factorLS).

$$CrA = 0.1 * ((-NDVI + 1)/2) \quad (6)$$

Box 4 shows the Java script used in GEE to obtain the C factor.

Box 1. *GEE code for cover management factor (C)*

```
var ndvi_median = ee.ImageCollection
("MODIS/006/MOD13A2").
median().multiply(0.0001).select('NDVI')
var factorC = ndvi_median.expression(
   '0.1 * ((- NDVI + 1) / (2))', {
     'NDVI': ndvi_median, });
```

P factor: The P-factor signifies comprehensive, overall effects of practices supporting conservation. It accounts for how surface environments distress flow paths and flow hydraulics. Presently, no major erosion control/support practices data of Tigray was available; henceforth it was given a value of 1.0 such that it had no effect on the design of soil loss.

2.6.2 Geostatistical Analysis

To predict the pattern of soil loss at kebele level in Tigray the Spatial Autocorrelation (Global Moran's I) tool was used. This tool calculates spatial autocorrelation based on both location and values of the features simultaneously. The pattern may be dispersed, clustered, or random, it depends on the location and the attribute values of the features. The Moran's I statistic for spatial autocorrelation is given as eq. 7 to 11.

$$\boldsymbol{I = \frac{n}{S_0} \frac{\sum_{i=1}^{n} \sum_{j=1}^{n} w_{i,j} z_i z_j}{\sum_{i=1}^{n} z_i^2}} \quad (7)$$

Where zi denotes the feature's attribute deviation from its average is the spatial weightage in between feature j and i, n is all number of features, and S_0 is the combination of all the spatial weights:

$$S_0 = \sum_{i=1}^{n} \sum_{j=1}^{n} w_{i,j} \quad (8)$$

The z_i-score for the statistic is computed as:

$$z_I = \frac{I - E[I]}{\sqrt{V[I]}} \quad (9)$$

Where:

$$E[I] = -1/(n-1) \quad (10)$$

$$V[I] = E[I^2] - E[I]^2 \quad (11)$$

To meet the third research objective ordinary least squire regression type was used (Eq. 12).

$$\gamma = \beta_0 + \beta_1 X_1 + \beta_2 X_2 + \beta_3 X_3 + \ldots\ldots \beta_n X_n + \varepsilon \quad (12)$$

Where γ is the dependent variable, β is coefficients, X is explanatory variables and ε is the random error.

To better understand how the factors are affecting the soil loss predictions Grouping Analysis tool was used to partition the kebele of Tigray (Eq. 13 & 14).

$$\text{Calinski} - \text{Harabasz pseudo F} - \text{statistic} = (R^2/n_c - 1)/(1 - R^2/n - n_c) \quad (13)$$

Where:

$$R^2 = \frac{SST - SSE}{\text{SST}} \quad (14)$$

In addition, SST is a reflection of between-group differences and SSE reflects within-group similarity:

$$\text{SST} = \sum_{I=1}^{nc} \sum_{k=1}^{ni} \sum_{j=1}^{nv} (V_{ij}^k - \overline{V^k})^2 \quad (15)$$

$$\text{SST} = \sum_{I=1}^{nc} \sum_{k=1}^{ni} \sum_{j=1}^{nv} (V_{ij}^k - \overline{V_i^k})^2 \quad (16)$$

Where

n = the number of features

n_i = the number of features in group t

n_c = the number of classes (groups)

n_v = the number of variables used to group features

V_{ij}^k = the value of the k[th] variable of the j[th] feature in the t[th] group

$\overline{V^k}$ = the mean value of the k[th] variable

$\overline{V_i^k}$ = the mean value of the kth variable in group i

3. RESULT

3.1 Precipitation runoff erosivity factor (R)

The predicted map of the annual R factor is given in appendix Figure 1. The min. and max. R is found 178.24 to 4329.05 respectively. The mean annual R in Eastern Tigray zone is 2478 with a standard deviation of 1069.

3.2 Soil erodibility factor (K)

The predicted map of the annual R factor is given in appendix Figure 2. The min. and max. K is found at 0.245 to 0.3558 respectively. The mean annual K in Tigray is 0.27 with a standard deviation of 0.01.

3.3 Slope length steepness factor (LS)

The predicted map of the annual LS factor is given in appendix Figure 3. The min. and max. LS is found 00 to 318523 respectively. The mean annual K in Eastern Tigray zone is 3607 with a standard deviation of 9046.

3.4 Cover management factor (C)

The predicted map of the annual C factor is given in appendix Figure 4. The min. and max. C is found at 0.020 to 0.046 respectively. The mean annual C in Eastern Tigray Zone was found 0.04.

3.5 Annual Soil Loss

The estimated soil loss in Tigray is shown in appendix Figure 5. The min. and max. Soil loss is found 00 to 7425130 t ha-1 year -1 respectively. The mean annual K in Eastern Tigray Zone is 65677 t ha-1 year -1 with a standard deviation of 144121.

3.6 Pattern of Soil loss at the kebele level

The result of autocorrelation for pattern analysis is given in Table 2 & appendix Figure 6, which indicates soil loss at the kebele level is highly clustered (z = 3.94).

Table 2. Global Moran's I Summary

Moran's Index:	**0.148521**
Expected Index:	-0.007692
Variance:	0.001568
z-score:	3.944822
p-value:	0.000080

3.7 Standard Residuals of Annual soil loss Prediction

As indicated appendix Figures 7 & 8 shows the map and histogram of Standard Residuals respectively. Table 3 & 4 shows the results of the model variables & OLS diagnostics. The multiple R2 was obtained as 0.70 from the ordinary least squared (OLS) regression model.

Table 3. OLS Results - Model Variables

Variable	Coefficient	Std Error	t-Statistic	Probability	Robust_SE	Robust_t	Robust_Pr	VIF
Intercept	446729.83	78704.50	5.67	0.000	71907.48	6.212	0.000000*	--------
C	940082.00	1159673.5	0.81	0.4190	1041922.70	0.902	0.368633	1.52001
K	-1961511.5	347615.20	-5.64	0.000	329113.78	-5.95998	0.000000*	1.458368
LS	15.03751	0.905789	16.60	0.000	1.240123	12.125	0.000000*	1.912069
R	25.58718	2.279686	11.22	0.000	2.562404	9.98562	0.000000*	1.952451

3.8. Groups of Annual soil loss Prediction

As indicated appendix Figures 9 & 10 shows the map of the groups of Annual soil loss Prediction & Parallel box plot chart respectively. Group numbers one and five are of special interest because of their outlier positions as shown in the Parallel box plot chart (appendix Figure 10).

Table 4. OLS Diagnostics

Input Features:	Kebele	Dependent Variable:	Est. Soil Loss Mean
No. of Observations:	131	Akaike's Information Criterion (AICc)	2930.81
Multiple R-Squared:	0.701	Adjusted R-Squared	0.69
Joint F-Statistic:	73.968	Prob(>F), (4659)	0.000000*
Joint Wald Statistic:	177.372	Prob(>chi-squared), (4)	0.000000*
Koenker (BP) Statistic:	42.608	Prob(>chi-squared), (4)	0.000000*
Jarque-Bera Statistic:	0.488	Prob(>chi-squared), (2)	0.784

4. DISCUSSION

Eastern Tigray zone is a very zig zag region; different types of topography are found here. Many researchers have also assessed soil erosion in Eastern Tigray zone. However, very less work is done on soil erosion at Kebele level in Eastern Tigray zone based on GIS. Estimates of soil removal by water show significant variation at the kebele level, this variation is a result of the variation in the distribution of different types of the soil, high flow accumulation, variations in vegetation cover, and finally spatial variation of rainfall. The R factor; which shows the impact of rainfall was calculated based on reliable rainfall data with quality control. Data record provides better information, especially in Africa (Brocca & others 2019). The K factor that is modeled in this study is also based on the full soil properties currently available. The same soil data was used by other researchers such as Viscarra et al. (2014) and de Brogniez et al (2015). The results are consistent with other scholars. Most areas of Tigray have a relatively small value of K. The vegetation data MOD13A2 used to calculate cover management was collected from the Google Earth engine archive. The same data has also been used by He et al. (2022); Wu et

al. (2022); Chabot et al. (2022); and He & others, (2022). The results were validated and published.

The OLS regression model was used to predict the significance of the factors; different tests are required to confirm the reliability of the OLS regression model. The modeled relationships are consistent because obtained statistic of Koenker is not statistically significant (p more than 0.005). The residuals show a Gaussian spatial pattern by the areal autocorrelation (Global Moran's I) analysis. Model predictions are unbiased because the Jarque-Bera Statistic test is also not statistically significant (p more than 0.01). There are no high intercorrelations among explanatory variables.

In the result of the grouping analysis Group, five has maximum mean soil loss, and this is primarily due to the high rainfall erosivity factor. The low soil loss in-group one is due to the low LS factor.

5. CONCLUSION

Smart techniques such as the GEE interface were used for erosivity factors of R, LS, C and K. In general, it was found that the soil erosion is high due high rainfall and zigzag topography in the Eastern Tigray zone, which equates to heavy annual soil losses over this area. The kebele that suffers from severe soil erosion occurs in areas having higher rainfall, more slope length and steepness (LS) factors; therefore, these areas should be further studied. GEE is useful for the estimation of soil removal. As it can process data input at any level, RUSLE can provide quantitative estimates of long-term soil removal in Eastern Tigray.

FUNDING

The authors did not receive support from any organization for the submitted work. The author certify that he has no affiliations with or involvement in any organization or entity with any financial interest or non-financial interest in the subject matter or materials discussed in this manuscript

REFERENCES

Abu Hammad, A., Lundekvam, H., & Børresen, T. (2004). Adaptation of RUSLE in the eastern part of the Mediterranean region. *Environmental Management*, *34*(6), 829–841. https://doi.org/10.1007/s00267-003-0296-7

Adigrat University. (2018). Adigrat city structural plan preparation (2018–2028), unpublished material

Ahmed Harb Rabia. (2012). GIS Spatial Modeling for Land Degradation Assessment in Tigray, Ethiopia. 161–166. https://sites.google.com/site/aharbrabia/services

Almagro, A., Thomé, T. C., Colman, C. B., Pereira, R. B., Marcato Junior, J., Rodrigues, D. B. B., & Oliveira, P. T. S. (2019). Improving cover and management factor (C-factor) estimation using remote sensing approaches for tropical regions. *International Soil and Water Conservation Research*, *7*(4), 325–334. https://doi.org/10.1016/j.iswcr.2019.08.005

Angima, S. D., Stott, D. E., O'Neill, M. K., Ong, C. K., & Weesies, G. A. (2003). Soil erosion prediction using RUSLE for central Kenyan highland conditions. *Agriculture, Ecosystems and Environment*, *97*(1–3), 295–308. https://doi.org/10.1016/S0167-8809(03)00011-2

Bagegnehu, B., Alemayehu, M., & Nigatu, W. (2019). Geographic Information System (GIS) based soil loss estimation using Universal Soil Loss Equation Model (USLE) for soil conservation planning in Karesa Watershed, Dawuro Zone, and South West Ethiopia. International Journal of Water Resources and Environmental Engineering, 11(8), 143–158. https://doi.org/10.5897/ijwree2018.0820..143-158

Biazin, B., Sterk, G., Temesgen, M., Abdulkedir, A., & Stroosnijder, L. (2012). Rainwater harvesting and management in rain fed agricultural systems in sub-Saharan Africa - A review. Physics and Chemistry of the Earth, 47–48, 139–151. https://doi.org/10.1016/j.pce.2011.08.015

Borrelli, P., Alewell, C., & Alvarez, P. (2021). CO. March. https://doi.org/10.31223/X5GS3T

Brocca, L., Filippucci, P., Hahn, S., Ciabatta, L., Massari, C., Camici, S., … Wagner, W. (2019). SM2RAIN–ASCAT (2007–2018): global daily satellite rainfall data from ASCAT soil moisture observations. Earth System Science Data, 11(4), 1583–1601. https://doi.org/10.5194/essd-11-1583-2019

Chabot, D., Stapleton, S., & Francis, C. M. (2022). Using Web images to train a deep neural network to detect sparsely distributed wildlife in large volumes of remotely sensed imagery: A case study of polar bears on sea ice. *Ecological Informatics*, *68*, 101547. https://doi.org/10.1016/J.ECOINF.2021.101547

Chen, H., Oguchi, T., & WU, P. (2017). Assessment for soil loss by using a scheme of alterative sub-models based on the RUSLE in a Karst Basin of Southwest China. *Journal of Integrative Agriculture*, *16*(2), 377–388. https://doi.org/10.1016/S2095-3119(16)61507-1

de Brogniez, D., Ballabio, C., Stevens, A., Jones, R. J. A., Montanarella, L., & van Wesemael, B. (2015). A map of the topsoil organic carbon content of Europe generated by a generalized additive model. European Journal of Soil Science, 66(1), 121-134.

Demirci, A., & Karaburun, A. (2012). Estimation of soil erosion using RUSLE in a GIS framework: A case study in the Buyukcekmece Lake watershed, northwest Turkey. *Environmental Earth Sciences*, *66*(3), 903–913. https://doi.org/10.1007/s12665-011-1300-9

Didan, K., Munoz, A. B., Solano, R., & Huete, A. (2015). *MODIS Vegetation Index User's Guide (MOD13 Series) Version 3.0 Ccollection 6)*. *2015*(May), 38.

Durigon, V. L., Carvalho, D. F., Antunes, M. A. H., Oliveira, P. T. S., & Fernandes, M. M. (2014). NDVI time series for monitoring RUSLE cover management factor in a tropical watershed. *International Journal of Remote Sensing*, *35*(2), 441–453. https://doi.org/10.1080/01431161.2013.871081

ESRI. (2013). The Language of Spatial Analysis. *Esri*, *36*(June), 1–49.

Esser, K., Vågen, T. G., Tilahun, Y., & Haile, M. (2002). Soil conservation in Tigray. Soil Conservation, 5, 1-21.

Evans, R., & Boardman, J. (2016). The new assessment of soil loss by water erosion in Europe. Panagos P. et al., 2015 Environmental Science & Policy 54, 438-447-A response. *Environmental Science and Policy*, *58*, 11–15. https://doi.org/10.1016/j.envsci.2015.12.013

Fiener, P., Neuhaus, P., & Botschek, J. (2013). Long-term trends in rainfall erosivity-analysis of high resolution precipitation time series (1937-2007) from Western Germany. *Agricultural and Forest Meteorology*, *171–172*, 115–123. https://doi.org/10.1016/j.agrformet.2012.11.011

Filho, W. L., & de Trincheria Gomez, J. (2017). Rainwater-smart agriculture in arid and semi-arid areas: Fostering the use of rainwater for food security, poverty alleviation, landscape restoration and climate resilience. Rainwater-Smart Agriculture in Arid and Semi-Arid Areas: Fostering the Use of Rainwater for Food Security, Poverty Alleviation, Landscape Restoration and Climate Resilience, December, 1–392. https://doi.org/10.1007/978-3-319-66239-8

Fitsum, H., John, P., & Nega, G. (2000). Land degradation in the Highlands of Tigray and Strategies for Sustainable Land Management. Policies for Sustainable Land Management in the Highlands of Ethiopia, 30(July 1999), 2–75.

Ganasri, B. P., & Ramesh, H. (2016). Assessment of soil erosion by RUSLE model using remote sensing and GIS - A case study of Nethravathi Basin. *Geoscience Frontiers*, *7*(6), 953–961. https://doi.org/10.1016/j.gsf.2015.10.007

Gebregziabher, et al. (2009). Contour furrows for in situ soil and water conservation, Tigray, Northern Ethiopia. Soil and Tillage Research, 103(2), 257–264. https://doi.org/10.1016/j.still.2008.05.021

Ghosal, K., & Das Bhattacharya, S. (2020). A Review of RUSLE Model. *Journal of the Indian Society of Remote Sensing*, *48*(4), 689–707. https://doi.org/10.1007/s12524-019-01097-0

Govers, G., & Moeyersons, J. (2005). Effectiveness of stone bunds in controlling soil erosion on cropland in the Tigray Highlands, northern Ethiopia. 287–297. https://doi.org/10.1079/SUM2005321

Hateffard, F., Mohammed, S., Alsafadi, K., Enaruvbe, G. O., Heidari, A., Abdo, H. G., & Rodrigo-Comino, J. (2021). CMIP5 climate projections and RUSLE-based soil erosion assessment in the central part of Iran. *Scientific Reports*, *11*(1). https://doi.org/10.1038/S41598-021-86618-Z

He, Y., Wang, L., Niu, Z., & Nath, B. (2022). Vegetation recovery and recent degradation in different karst landforms of southwest China over the past two decades using GEE satellite archives. *Ecological Informatics*, *68*, 101555. https://doi.org/10.1016/J.ECOINF.2022.101555

Kaygusuz, K. (2011). Energy services and energy poverty for sustainable rural development. Renewable and Sustainable Energy Reviews, 15(2), 936–947. https://doi.org/10.1016/j.rser.2010.11.003

Kinnell, P. I. A. (2014). Applying the RUSLE and the USLE-M on hillslopes where runoff production during an erosion event is spatially variable. *Journal of Hydrology*, *519*(PD), 3328–3337. https://doi.org/10.1016/j.jhydrol.2014.10.016

Kouli, M., Soupios, P., & Vallianatos, F. (2009). Soil erosion prediction using the Revised Universal Soil Loss Equation (RUSLE) in a GIS framework, Chania, Northwestern Crete, Greece. *Environmental Geology*, *57*(3), 483–497. https://doi.org/10.1007/s00254-008-1318-9

Kuria, A. W., Barrios, E., Pagella, T., Muthuri, C. W., Mukuralinda, A., & Sinclair, F. L. (2018). Farmers ' knowledge of soil quality indicators along a land degradation gradient in Rwanda Geoderma Regional Farmers ' knowledge of soil quality indicators along a land degradation gradient in Rwanda. Geoderma Regional, December, e00199. https://doi.org/10.1016/j.geodrs.2018.e00199

Liu, K., Tang, G., Jiang, L., Zhu, A. X., Yang, J., & Song, X. (2015). Regional-scale calculation of the LS factor using parallel processing. *Computers and Geosciences*, *78*, 110–122. https://doi.org/10.1016/j.cageo.2015.02.001

Luvai, A., Obiero, J., & Omuto, C. (2022). Soil Loss Assessment Using the Revised Universal Soil Loss Equation (RUSLE) Model. Applied and Environmental Soil Science, 2022. https://doi.org/10.1155/2022/2122554

Megerssa, G. R., & Bekere, Y. B. (2019). Causes, consequences and coping strategies of land degradation: Evidence from Ethiopia. Journal of Degraded and Mining Lands Management, 7(1), 1953–1957. https://doi.org/10.15243/jdmlm.2019.071.1953

Mekuria, W., Veldkamp, E., Haile, M., Gebrehiwot, K., Muys, B., & Nyssen, J. (2009). Effectiveness of exclosures to control soil erosion and local community perception on soil erosion in Tigray, Ethiopia. African Journal of Agricultural Research, 4(4), 365–377.

Mitasova, H., Barton, M., Ullah, I., Hofierka, J., & Harmon, R. S. (2013). GIS-Based Soil Erosion Modeling. In Treatise on Geomorphology (Vol. 3, Issue November 2017). https://doi.org/10.1016/B978-0-12-374739-6.00052-X

Moges, D. M., & Bhat, H. G. (2017). Integration of geospatial technologies with RUSLE for analysis of land use/cover change impact on soil erosion: case study in Rib watershed, north-western highland Ethiopia. Environmental Earth Sciences, 76(22), 1–14. https://doi.org/10.1007/s12665-017-7109-4

Nyssen, J., Clymans, W., Descheemaeker, K., Poesen, J., Vandecasteele, I., Vanmaercke, M., Zenebe, A., Van Camp, M., Haile, M., Haregeweyn, N., Moeyersons, J., Martens, K., Gebreyohannes, T., Deckers, J., & Walraevens, K. (2010). Impact of soil and water conservation measures on

catchment hydrological response-a case in north Ethiopia. Hydrological Processes, 24(13), 1880–1895. https://doi.org/10.1002/hyp.7628

Panagos, P., Meusburger, K., Ballabio, C., Borrelli, P., & Alewell, C. (2014). Soil erodibility in Europe: A high-resolution dataset based on LUCAS. *Science of the Total Environment*, *479–480*(1), 189–200. https://doi.org/10.1016/j.scitotenv.2014.02.010

Rockström, J., & Falkenmark, M. (2015). Agriculture: Increase water harvesting in Africa. Nature, 519(7543), 283–285. https://doi.org/10.1038/519283a

Schmidt, S., Tresch, S., & Meusburger, K. (2019). Modification of the RUSLE slope length and steepness factor (LS-factor) based on rainfall experiments at steep alpine grasslands. *MethodsX*, *6*, 219–229. https://doi.org/10.1016/j.mex.2019.01.004

Sileshi, M., Kadigi, R., Mutabazi, K., & Sieber, S. (2019). Determinants for adoption of physical soil and water conservation measures by smallholder farmers in Ethiopia. *International Soil and Water Conservation Research*, *7*(4), 354–361. https://doi.org/10.1016/j.iswcr.2019.08.002

Tadesse, A., Gebrelibanos, T., & Geberehiwot, M. (2016). Characterization and Impact Assessment of Water Harvesting Techniques : A Case Study of Abreha Weatsbeha Watershed , Tigray , Ethiopia . 1–28.

Tanyaş, H., Kolat, Ç., & Süzen, M. L. (2015). A new approach to estimate cover-management factor of RUSLE and validation of RUSLE model in the watershed of Kartalkaya Dam. *Journal of Hydrology*, *528*, 584–598. https://doi.org/10.1016/j.jhydrol.2015.06.048

Teka, K., Haftu, M., Ostwald, M., & Cederberg, C. (2020). Can integrated watershed management reduce soil erosion and improve livelihoods? A study from northern Ethiopia. International Soil and Water Conservation Research, 8(3), 266–276. https://doi.org/10.1016/j.iswcr.2020.06.007

Tesfahunegn, G. B., & Gebru, T. A. (2020). Variation in soil properties under different cropping and other land-use systems in Dura catchment, Northern Ethiopia. PloS one, 15(2), e0222476.

Tian, P., Zhu, Z., Yue, Q., He, Y., Zhang, Z., Hao, F., Guo, W., Chen, L., & Liu, M. (2021). Soil erosion assessment by RUSLE with improved P factor and its validation: Case study on mountainous and hilly areas of Hubei Province, China. *International Soil and Water Conservation Research*, *9*(3), 433–444. https://doi.org/10.1016/j.iswcr.2021.04.007

Van Remortel, R. D., Hamilton, M. E., & Hickey, R. J. (2001). Estimating the LS factor for RUSLE through iterative slope length processing of digital elevation data within arclnfo grid. *Cartography*, *30*(1), 27–35. https://doi.org/10.1080/00690805.2001.9714133

Vancampenhout, K., Nyssen, J., Gebremichael, D., Deckers, J., Poesen, J., Haile, M., & Moeyersons, J. (2006). Stone bunds for soil conservation in the northern Ethiopian highlands: Impacts on soil fertility and crop yield. Soil and Tillage Research, 90(1–2), 1–15. https://doi.org/10.1016/j.still.2005.08.004

Viscarra Rossel, R. A., Webster, R., Bui, E. N., & Baldock, J. A. (2014). Baseline map of organic carbon in Australian soil to support national carbon accounting and monitoring under climate change. *Global Change Biology*, *20*(9), 2953-2970.

Waters, N. (2012). A Review of "Handbook of Applied Spatial Analysis: Software Tools, Methods and Applications." In *Annals of the Association of American Geographers* (Vol. 102, Issue 1). https://doi.org/10.1080/00045608.2011.624965

Wilken, F., Fiener, P., Ketterer, M., Meusburger, K., Muhindo, D. I., Van Oost, K., & Doetterl, S. (2020). Assessing soil erosion of forest and cropland sites in wet tropical Africa using 239+ 240 Pu fallout radionuclides. *Soil Discussions*, *2020*, 1-22.

Wu, T. Y., Yeh, K. T., Hsu, H. C., Yang, C. K., Tsai, M. J., & Kuo, Y. F. (2022). Identifying Fagaceae and Lauraceae species using leaf images and convolutional neural networks. *Ecological Informatics*, *68*, 101513. https://doi.org/10.1016/J.ECOINF.2021.101513

Xu, L., Xu, X., & Meng, X. (2013). Risk assessment of soil erosion in different rainfall scenarios by RUSLE model coupled with Information Diffusion Model: A case study of Bohai Rim, China. *Catena*, *100*, 74–82. https://doi.org/10.1016/j.catena.2012.08.012

Yue, T., Xie, Y., Yin, S., Yu, B., Miao, C., & Wang, W. (2020). Effect of time resolution of rainfall measurements on the erosivity factor in the USLE in China. *International Soil and Water Conservation Research*, *8*(4), 373–382. https://doi.org/10.1016/j.iswcr.2020.06.001

Zerssa, G., Feyssa, D., Kim, D., & Eichler-löbermann, B. (2021). Challenges of Smallholder Farming in Ethiopia and Opportunities by Adopting Climate-Smart Agriculture. 1–25.

Appendices

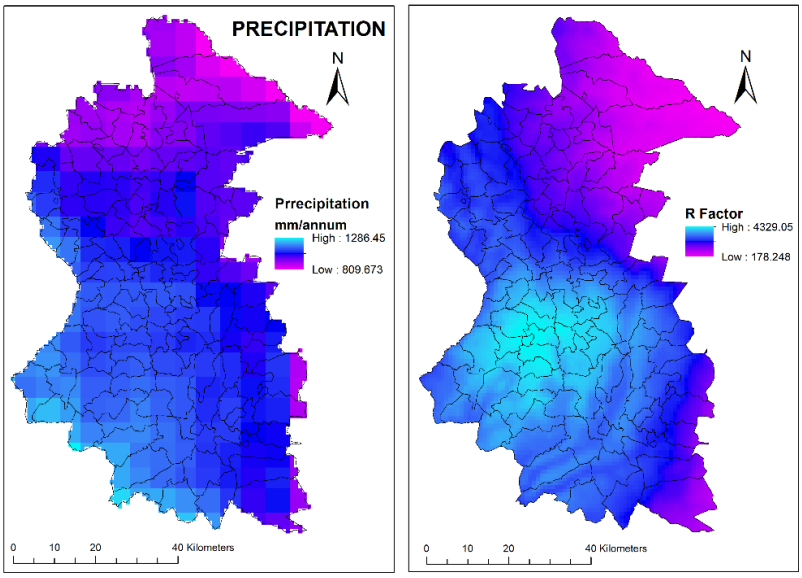


Figure 1. Erosivity factor R

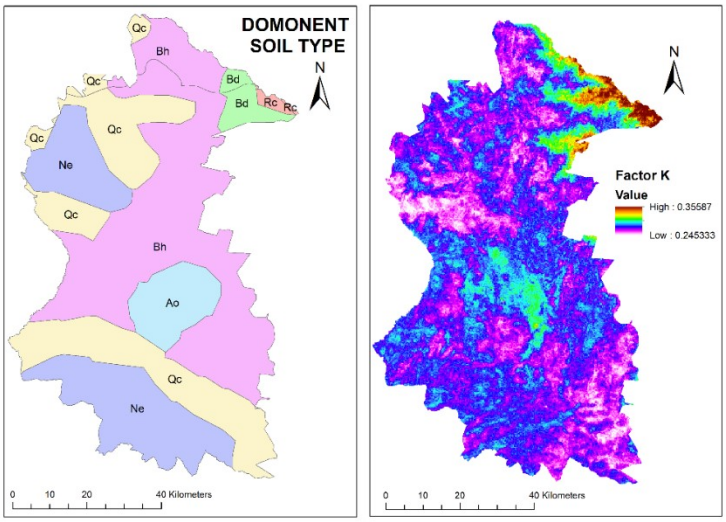


Figure 2. Erosivity factor K

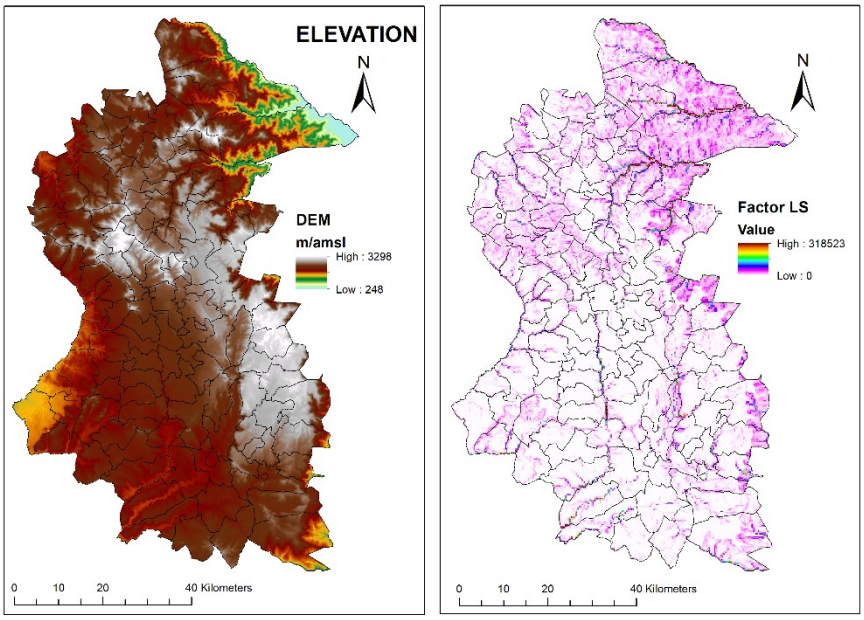


Figure 3. Erosivity factor LS

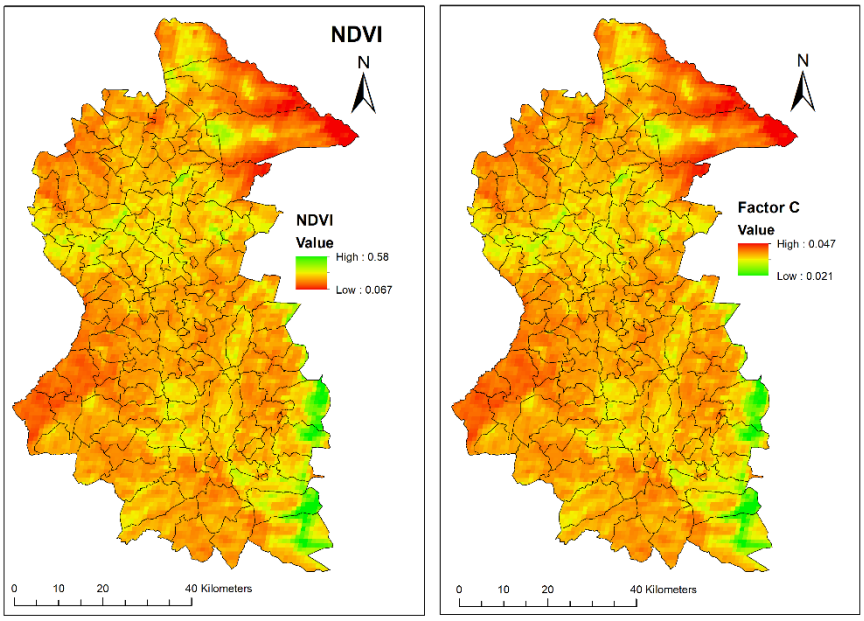


Figure 4. Erosivity factor C

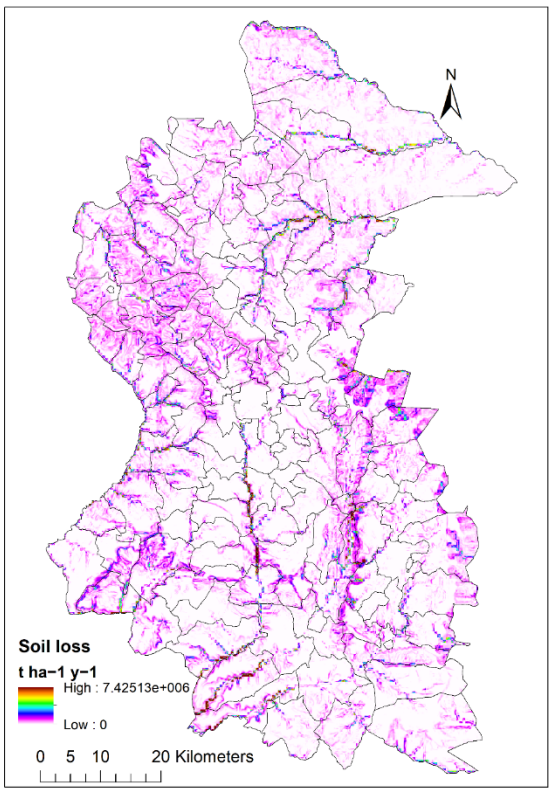


Figure 5. Estimated Annual soil erosion

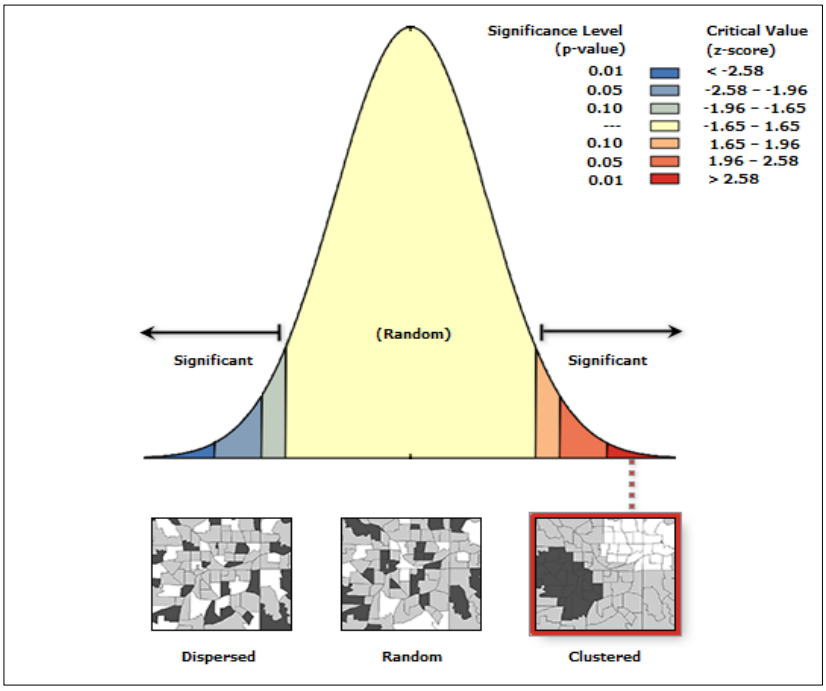


Figure 6. Pattern at Kebele level

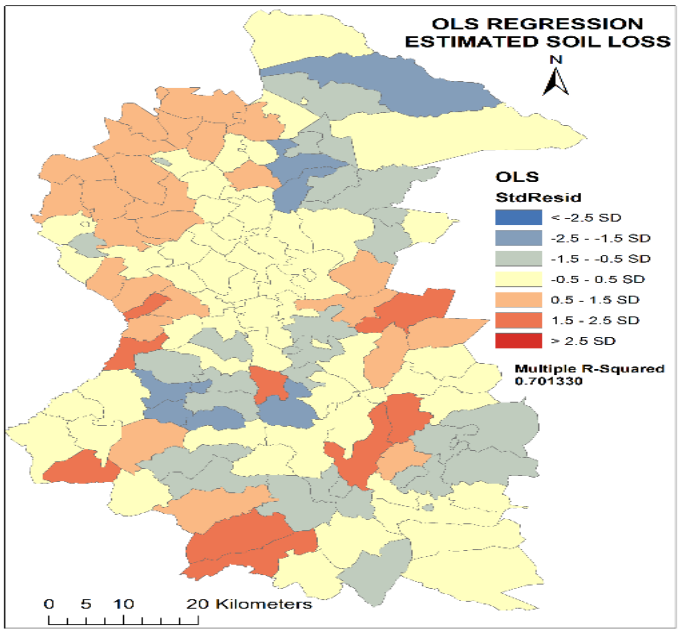


Figure 7. Standard Residual Map

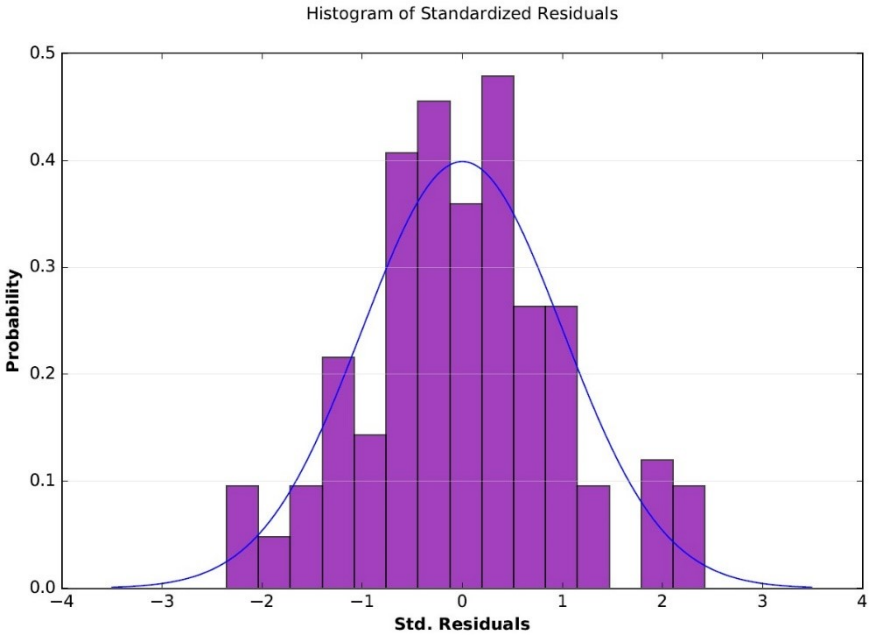


Figure 8. Histogram of residuals

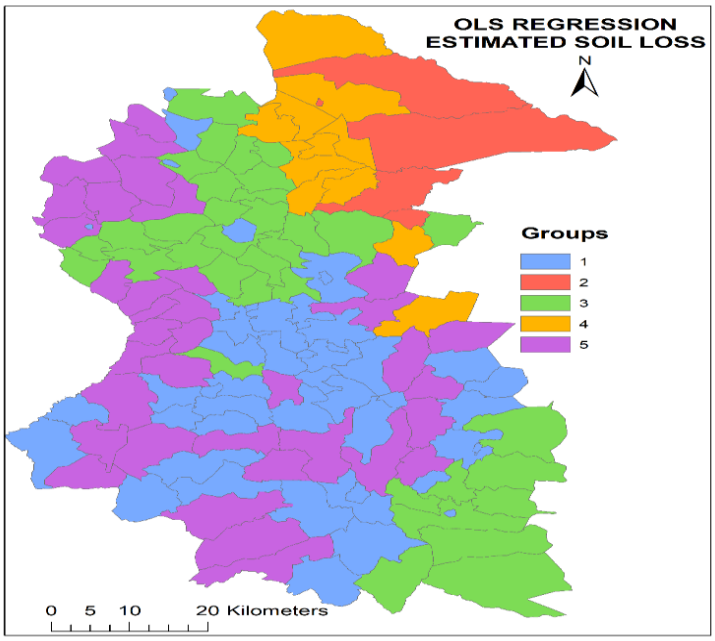


Figure 9. Groups of Annual soil loss Prediction

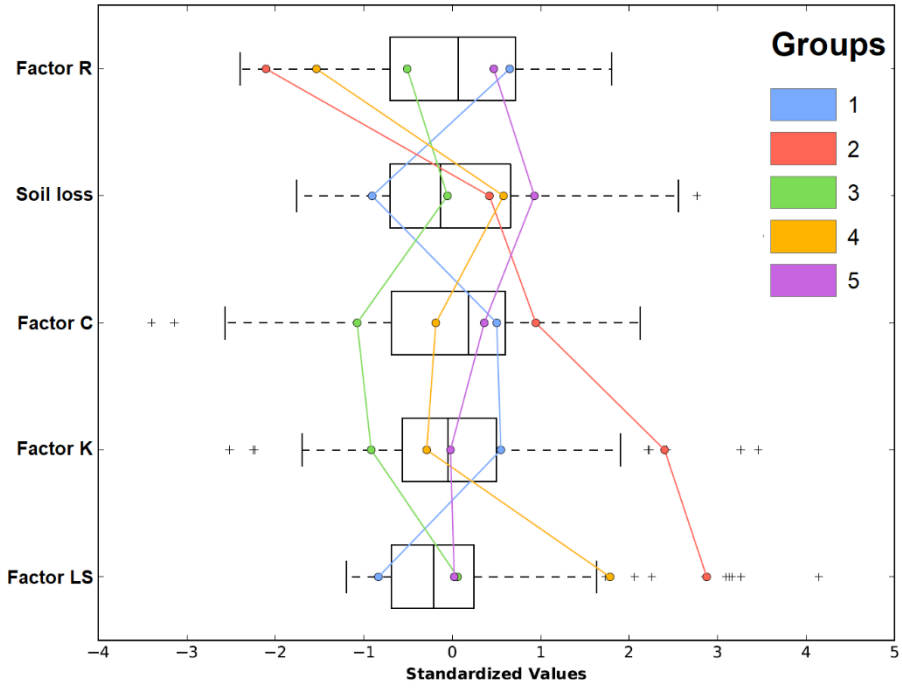


Figure 10. Parallel Box Plot

Publisher's Note

Daagu International Journal of Basic and Applied Research remains neutral with regard to jurisdictional claims in published maps and institutional affiliations.